INVESTIGATION OF THE FERMI SURFACE IN MOLYBDENUM ON THE BASIS OF THE RADIO FREQUENCY SIZE EFFECT

V. V. BOĬKO, V. A. GASPAROV, and I. G. GVERDTSITELI

Submitted August 27, 1968

Zh. Eksp. Teor. Fiz. 56, 489–500 (February, 1969)

The radio-frequency size effect was studied, at frequencies 3–20 MHz and temperatures 1.7–4.2°K, in thin, plane-parallel plates of molybdenum. The anisotropy of the extremal dimensions of the Fermi surface was investigated in the three crystallographic planes (110), (111), and (121). The data obtained made it possible to determine both the shape and the dimensions of the electron and the hole surfaces. Identification of the observed cross sections was made with account of the dependence of the lines of the size effect on the slope of the magnetic field relative to the surface of the sample and the polarization of the high frequency field. The complicated form of the isoenergetic surface of the electrons leads to the appearance of a number of size effect lines, due to the presence of breaks in the electron trajectories in the magnetic field. No lines have been observed which support the idea of an open Fermi surface; this confirms the existence of a gap between the hole octahedron and the electron "jack." The mean current carrier velocities in the central part of the electron and hole surfaces can be determined from the results and are $v_e = 0.60 \times 10^8$ cm/sec and $v_h = 0.89 \times 10^8$ cm/sec, respectively.

INTRODUCTION

AT the present time, rich experimental material has been collected and the basic principles of the calculation of Fermi surfaces of nontransition metals are comparatively clear. The study of the electron spectrum of the transition metals can be regarded as the next more difficult problem both in the experimental and in the theoretical sphere. The experimental difficulties are occasioned by the fact that the transition metals generally have a higher melting point and are difficult to obtain in sufficiently pure form.

At the present time, the most investigated of the group is chromium. However, none of the metals, even of this group, has been investigated as completely as many of the nontransition metals.

From measurement of the surface resistance under conditions of the anomalous skin effect[1] and from data on the magnetoresistance of single crystal samples[2,3] it has been established that the electron structure of Cr, W, and Mo cannot be described within the framework of the nearly free electron model. In 1962, Lomer,[4,5] basing his argument on the assumption that the s-d energy bands of the chromium group are similar to the energy bands of iron, which were considered previously,[6] suggested a single model of the Fermi surface for these metals. The experimental results of the investigations of the de Haas–van Alphen effect, carried out in comparatively weak magnetic fields by Brandt and Rayne[7] on Cr, W, Mo, and the experiments on the study of the size effect in tungsten[8] were seen to be in qualitative agreement with the theoretical model.

The most detailed experimental evidence on the study of the de Haas–van Alphen effect in molybdenum and their comparison with the Lomer model are contained in the work of Sparlin and Marcus.[9] However, it must be noted that information relative to the large cross sections of the electron and hole Fermi surfaces of molybdenum is comparatively small in this research. It is not possible to draw any final conclusions on the shape and the dimensions of these cross sections from the existing fragmentary experimental data known from the magnetoacoustic measurements of Jones and Rayne[10,11] and from the results on the measurement of the de Haas–van Alphen effect of Myers and Leaver,[12] and also of Girvan and Gold.

In 1965, Loucks[13] made a direct calculation of the Fermi surface of molybdenum by the method of augmented plane waves, and obtained results which permitted a quantitative comparison with experiment. In this connection, it was of interest not only to get new experimental data relative to the large cross sections of the Fermi surface of molybdenum, but also to make a detailed study of the entire surface by one independent method—with the help of the radio-frequency size effect.[14,15]

A preliminary communication of these investigations was published in [16]. In the present work we report the results of subsequent experiments.

EXPERIMENT

The radio-frequency size effect makes it possible to fix those values of the magnetic field for which the characteristic dimensions of the extremal trajectories are comparable with the thickness of the monocrystalline plates. This makes it possible to obtain data on the Fermi surface.

In particular, for the extremal cross sections in a field parallel to the surface of the metal, the size of the 2p electron orbit in momentum space in the $\mathbf{n} \times \mathbf{H}$ direction is equal to

$$2p = \frac{e}{c} Hd, \tag{1}$$

where H is the value of the magnetic field determined by experiment, d the thickness of the plate, e the

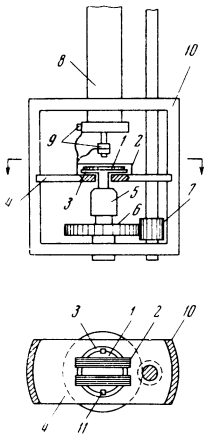

FIG. 1. Scheme for location of specimen in the coil of the generator.

charge on the electron, c the velocity of light, and n the normal to the surface of the sample.

The modulation method of measurement of the dependence of the active part of the surface impedance of the metallic sample on the magnetic field was used in the experiments. The measuring generator employed the circuit of Hopkins.[17] The working regime of the generator was established close to the threshold. The frequency range was chosen in the interval 3–20 MHz, while the modulation frequency was 38 Hz.

Sample 1 (Fig. 1) was placed inside the coil 2, which consisted of two sections. Each of these sections had 20 turns of copper wire of diameter 50 microns, wound in a single layer. The sample lay freely on a quartz support 3, the leg of which passed through an opening in the quartz plane 4 and was fastened by the clamp 5.

Since the intensity of the size-effect lines depends on the polarization of the electric field, to increase the sensitivity of the method, provision was made for rotation of the magnet in the plane of the sample and rotation of the sample by means of the gear train 6–7. The coaxial line 8 and the adjustable contacts 9 served to connect the coil 2 with the rest of the high-frequency generator circuit, which was maintained at room temperature. The plate 4 was fixed in the brass frame 10. The sample was glued to the support 3 with strips of tissue paper.

The magnetic field was measured in our experiments from the signals of nuclear resonance from protons which were recorded simultaneously with the recording of the derivative of the real part of the surface impedance of molybdenum. The samples were cut by an electric spark saw out of single crystalline rods of diameter ~6 mm, passing through multiple electron-beam zone refining. The ratio of electrical resistances for these rods R(300°K)/R(4.2°K) = 18 000. Plane parallel disks of thickness ~0.4–0.5 mm and surface purity ∇7 were then etched down to the thickness necessary for experiment (~0.24 mm) in a special etching solution (30% H_2SO_4, 30% HNO_3, 30% H_3PO_4 and 10% H_2O).

Control of the orientation of the samples was done by x-ray means with an accuracy to within 30′ and their thickness was measured by means of a vertical optimeter IZV-2. One should note the great hardening of the samples used, which materially simplified working with them and made it possible to increase the accuracy of measurement of the thickness to within 1 micron. The scatter in the thickness for each sample did not exceed 2 microns (less than 1%).

EXPERIMENTAL RESULTS

Sample recordings of the size-effect lines observed in the (110) and (111) planes for a field **H** parallel to the surface of the samples are shown in Figs. 2 and 3. The majority of the experiments on which we are reporting were performed at 4.2°K, since lowering of the temperature from 4.2 to 1.7°K had little effect on the amplitude of the size effect lines, because of the high Debye temperature of molybdenum (Θ = 425°K).

The angular dependences of the position of the lines were investigated on samples the normals **n** to the

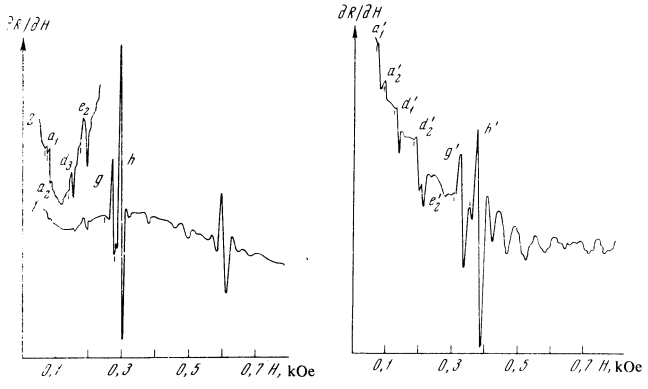

FIG. 2. Recording of the size effect lines for a sample with n||[110], d = 0.239 mm, T = 4.2°K, f = 3.8 MHz, ∠(H, [001]) = 50°. The primes denote values of the field used for the calculations. The scale for curve 2 is enlarged by a factor of five. The lines for h were due to a chain of orbits.

FIG. 3. Recording of the size effect lines for a sample with n||[111], d = 0.227 mm, T = 4.2°K, f = 3.8 MHz, H||[$\bar{1}\bar{1}$2]

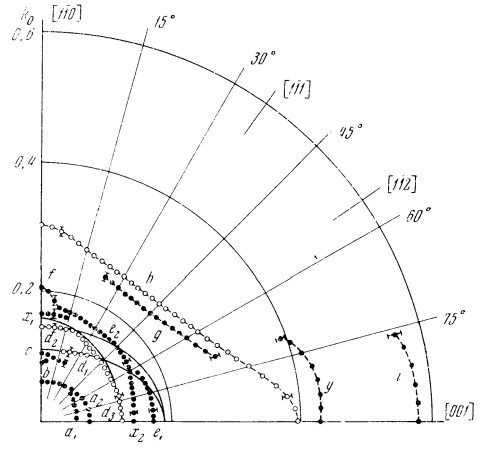

FIG. 4. Angular dependence of the half-width of extremal orbits (in units of k_0) in the (110) plane. The lines from the orbits on the electron and hole surfaces are indicated by ● and ○, respectively. The solid lines are the shadow projections of the ellipsoids on this plane.

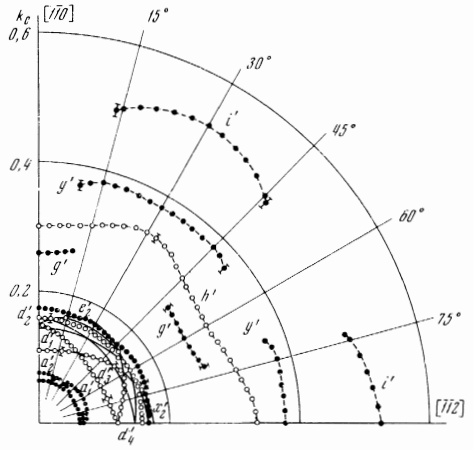

FIG. 5. Experimental results in the (111) plane. The notation is the same as in Fig. 4.

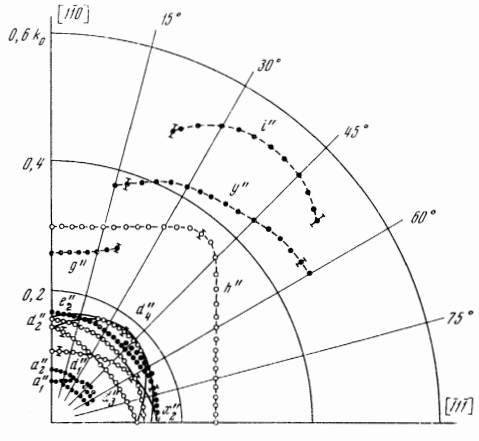

FIG. 6. Experimental results in the (121) plane. The notation is the same as in Fig. 4.

surfaces of which were identical with the following crystallographic directions: $\mathbf{n} \parallel [110]$, $\mathbf{n} \parallel [111]$, $\mathbf{n} \parallel [121]$.

The results are shown in Figs. 4–6, where the quantity k is marked off in units of k_0 as a function of direction in which the size was measured. The value $k = p/\hbar$ was determined from Eq. (1), while k_0 is the limiting wave vector of the Brillouin zone in the [100] direction ($k_0 = 2\pi/a = 1.998$ Å^{-1}, a is the lattice constant of molybdenum at helium temperatures). On these diagrams, the lines due to electron orbits on one and the same parts of the Fermi surface have the same letter designation, while the primes denote only their belonging to some plane.

The lines from transverse orbits were not plotted on the diagram. The value of the field H necessary for calculation in Eq. (1) was taken from the left edge of the lines.[18,19] The roughness of the absolute measurement of the wave vector is determined by the error in the measurement of the thickness of the samples (~1%) and the error in the measurement of the field (~1–4%), which was due to insufficiently clear beginning of the series of lines. For the lines g, h, i, the error amounted to ±2%, and ±(3–5)% for the others.

For each of the lines in Figs. 4–6, the values were obtained from the results of measurements on several samples; however, in order not to make the picture too complicated, we did not put in the special designations corresponding to each of them. The total number of samples studied by us was ten.

All the values of k were determined for **H** parallel to the surface of the samples, for two polarizations of the electric and magnetic fields: $\mathbf{E}_\sim \parallel \mathbf{H}$ and $\mathbf{E}_\sim \perp \mathbf{H}$. The lines g, h, and f were observed for $\mathbf{E}_\sim \parallel \mathbf{H}$. As studies in an oblique field showed, only the f line is split when the field is inclined to the surface; all the remaining lines were not split up to angles of inclination of the field of ±10°.

The presence of a large number of lines in fields up to 200 Oe made deciphering of the experimental data more difficult. First, these lines were located, for a number of directions of the magnetic field, at very small distances from one another (in the field), which did not allow us to separate them sufficiently sharply; second, some lines from the chain of orbits were superimposed on the lines corresponding to the basic trajectories of the electrons. For example, in the (121) plane (Fig. 6) along the [$\bar{1}$1$\bar{1}$] direction a line should be seen from the orbits of electrons on the electron octahedron and two spheres; however, because of the intense lines from the chain of orbits, it was not possible to observe them.

It was possible to resolve the lines g and h in the (110) plane (Fig. 4) with increasing frequency, but only in samples whose thickness was greater than 0.2 mm. This is explained by the fact that part of the experimental points in the angular range $\sphericalangle(\mathbf{H}, [1\bar{1}0]) = 0–20°$ and $\sphericalangle(\mathbf{H}, [001]) = 0–24°$ was referred to the electron "jack" (cf. Fig. 2 from [16] with Fig. 4 of the present research). It was not possible to increase the thickness of the samples used in the initial stage of our investigations, because of insufficient purity of the original material.

DISCUSSION OF RESULTS

The model of the Fermi surface of molybdenum suggested by Lomer and Loucks[13] is shown in Fig. 7. It is closed, completely compensated and consists of the following surfaces: a) electron surface ("jack") with

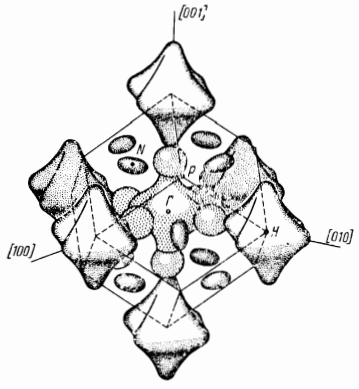

FIG. 7. Fermi surface of molybdenum.

lenses located at the point Γ of the Brillouin zone. This surface can be regarded as a shaped octahedron which intersects with six spheroids. The intersection of the ends of the octahedron with the spheroids gives the lens along ΓH; b) the hole octahedron with a center of symmetry at the point H; c) six hole ellipsoids at N, the principal axes of which are located along NP ([001]), NΓ ([110]), NH ([110]). The electron "jack"; in accord with the model, it comes in contact with the hole octahedron.

All the above surfaces are well described by lines observed experimentally. The simplest of these surfaces are the hole octahedron and the ellipsoids. We shall begin our discussion of the results with them.

1. Hole octahedron at H. The lines h, h′, h″ (Figs. 4–6) can evidently be uniquely connected with orbits on the hole octahedron with center of symmetry at the point H of the Brillouin zone. This is supported both by the angular dependence of the location of the lines and by the existence of lines over the entire angular range.

In connection with the fact that the size effect gives a shadow projection of the Fermi surface on a plane perpendicular to the normal to the sample, this projection will be identical with the cross section of the Fermi surface only for the sample in the (110) plane. The behavior of the h line in the diagram of Fig. 4 accurately describes this cross section, which allows us to determine the basic dimensions of the octahedron. They are in complete agreement with the results obtained from the diagrams of Figs. 5 and 6. The numerical values of these dimensions are given in the table.

The extremal cross sectional areas of the octahedron in the (100), (110), and (111) planes, computed from the given data, $-S_{(100)} = 1.5$ Å^{-2}, $S_{(110)} = 1.08$ Å^{-2}, $S_{(111)} = 1.01$ Å^{-2} agree, within the limit of error of the experiment, with the values determined in [9,12].

For $\mathbf{H} \parallel [111]$, the orbit of the holes on the central part of the hole octahedron is a hexagon with rounded corners. The velocity of the holes on this orbit changes its direction six times, while the mean drift velocity over one period along the field is equal to zero. The maximum angle which it makes with the plane of the orbit is equal to 19° 18′ in momentum space. Therefore this trajectory of holes in coordinate spaces does not lie in the plane perpendicular to the direction of the magnetic field, which explains the existence of the h lines for $\mathbf{E} \parallel \mathbf{H}$.

Knowing the length of such an orbit and using the value of the effective mass on it from [20], we computed the mean velocity of the holes according to the formula

$$\bar{v} = \frac{\hbar k}{2\pi m^*} |\cos 19°18'|^{-1}, \qquad (2)$$

where $\hbar k = p$ is the length of the orbit in momentum space, and m^* is the effective mass of the holes. Hence $\bar{v}_h = 0.89 \times 10^8$ cm/sec.

Knowledge of the basic dimensions and shape of the cross section of the octahedron allows us to compute the area of its surface and its volume with account of the rounding of the corners and of the edges: $S = 5.0$ Å^{-2}, $V = 0.90$ Å^{-3}.

2. Hole ellipsoids at N. We relate the lines of the groups d, d′, d″ on the diagrams of Figs. 4–6 to orbits on hole ellipsoids at the points N of the Brillouin zone. Such an interpretation is based on the angular dependence and location of the lines on the diagram. According to the model from [5,13] the ellipsoids are extended along the [100] directions and compressed along [110]. As is seen from the diagrams, the experimental results allow us to determine all three principal semiaxes of the ellipsoids a, b, and c (see the table). Using these values and knowing the position of the ellipsoids in the Brillouin zone, we can construct their shadow projections in the corresponding plane. They are drawn on the diagrams as continuous lines. With the exception of the line d_3 (Fig. 4), all the experimental points describe these projections satisfactorily.

Experimental and theoretical values of the k-vectors of the Fermi surface of molybdenum (in Å^{-1})

Surface	Details	Theory [13]	Experiment: Present work	Experiment: Other investigations
Electron "jack" and lenses	[100]	1.149	1.16	1.2 [11]
	[121]	—	0.49	0.48 [13]
	[111]	0.438	0.47	
	[110]	0.486	0.52	
	Distance from Γ to the plane of the neck		0.58	
	Radius of the spheroid	0.32	0.35	0.365 [9]
	Diameter of the neck	0.37	0.36	0.383 [9]
	Diameter of the spheroid		0.31	0.32 [9]
	Dimension of the lens along ΓH		0.22	
Holes in H	[100]	0.841	0.79	
	[121]		0.54	
	[111]	0.533	0.51	
	[110]	0.627	0.60	0.60 [11]
Holes in N	[100] a =	0.368	0.38	0.39 [9]
	[110] b =	0.266	0.29	0.30 [9]
	[110] c =	0.189	0.22	0.23 [9]

The departure of the line d_3 lies within the limits of error of the experiment and can be connected with the indeterminacy in the choice of the reference point because of the strong, nonmonotonic dependence of the impedance on the value of the magnetic field. The insufficiently complete character of the dependence of the shadow projections can explain the weak intensity of the size-effect lines, due to the significant curvature of the corresponding portions of the Fermi surface and the difficulty of their resolution. Furthermore, for a number of directions of the magnetic field, lines from the orbits of electrons on spheroids are superimposed on these lines. Despite this, the anisotropy of the lines of the groups d, d′, and d″ allows us to draw an unambiguous conclusion relative to the shape and size of the hole ellipsoids at N.

The total area of the surface of the six ellipsoids, computed from these results, is $S = 6.6$ Å^{-2}, while their volume is $V = 0.61$ Å^{-3}.

3. Electron "jack" and lenses. Let us now proceed to the electron Fermi surface of molybdenum. This surface is more complicated. The large number of lines which are observed experimentally testifies to this. We shall relate all the remaining lines in Figs. 4–6 to this surface.

As has already been noted, upon rotation of the magnetic field relative to the crystallographic directions in the (110) plane, the lines of the experimental points from the extremal orbits of the electron "jack" will

give directly the section of this surface with the (110) plane (Fig. 4). Such lines are first of all the lines i and g. The angular range of observation of these lines and their significant intensity gives evidence that they belong to orbits of electrons on the octahedron and two spheres and on the central part of the electron "jack." The intensity of the g line is maximal when the magnetic field is directed along the $[1\bar{1}2]$ direction, while that of the i line, for the direction of the magnetic field along $[1\bar{1}0]$. This can easily be explained if we take it into account that for these directions of the magnetic field the trajectory of the electrons enters into the skin layer with plane portions. The line i disappears at an angle 14° to the [001] direction. We could not discern the moment of appearance of the g line, since lines in the twin field from the trajectory x_2 were superposed on this line in the angular range 17–20° from the [001] direction. In this connection, the experimental points corresponding to the line g begin with an angle 20° to the [001] direction, and continue to 66°.

At a direction close to the $[1\bar{1}0]$ direction, a line was observed behind the h line which could be due to orbits on the electron octahedron and the four spheroids; however, since it coincided in position with the lines from the chain of orbits, it was not drawn in the diagram.

The existence of the lines e_1 and e_2 and their anisotropy can be explained by the orbits of electrons on the spheroids. The radius of these spheroids is determined by the lines e_1 along the [001] direction. The value for the radius of the spheroids obtained from the results of measurements in the (111) plane agrees with this value (the size of e_2' along $[1\bar{1}0]$).

The line f belongs to the noncentral cross section of the electron "jack" and is most probably due to the orbit which runs around the bridges between the four spheres. The line b is absent in the (111) and (121) planes and exists in the (110) plane in the angular range 0–3° from the $[1\bar{1}0]$ direction. The angular interval of its existence and its relatively weak intensity leave no doubt that it is due to orbits on the neck of the electron "jack."

Proof for the existence of electron lenses along ΓH in molybdenum can be obtained from the presence of lines of the groups a, a′, a″ in weak fields. The sizes of the lenses along the basic crystallographic directions were determined by us in a study of the anisotropy of these lines in all three planes. The absence of experimental points for the line a″ in the (121) plane in the angular range 0–30° from the $[\bar{1}1\bar{1}]$ direction is explained by the strong nonmonotonic dependence of the surface impedance Z of molybdenum, which is superimposed on these lines at the corresponding directions of the magnetic field.

It is well known that for a complicated form of the electron trajectories, the appearance of the size-effect lines can be due to the presence of breaks in these trajectories. Such lines were observed experimentally by Gantmakher and Krylov in the study of the Fermi surface of tin[21] and indium.[18]

For molybdenum, the breaks on the electron trajectories can exist for directions of the magnetic field close to the [110] and [001] directions. For these directions of the magnetic field, the measured dimensions of the central cross sections of the electron "jack" are shown in Fig. 8. To the lines due to breaks on the diagrams of Figs. 4–6, we assign the lines x_1, x_2, y, x_2', y′, x_2'', y″. Such an origin of these lines seems to us the only one possible. The most interesting

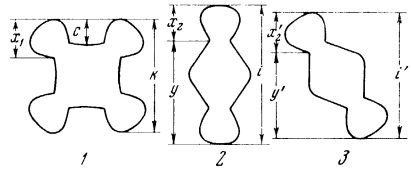

FIG. 8. Measured dimensions of the central cross section of the electron "jack:" 1 – (110) plane, H||[001]; 2 – (110) plane, H||$[1\bar{1}0]$; 3 – (111) plane, H||[110].

of them is the line x_2. This line determines the size from the end of the electron "jack" to its neck. From the relative width of this line, $\Delta H/H \sim 8\%$, we can estimate the radius of the neck circumference: $\Delta H/H \geq \Delta k/k$, where Δk is the radius of the neck and k is the corresponding size of the electron orbit, equal to 0.58 Å^{-1}. It then follows that the radius of the neck is $\Delta k \lesssim 0.046$ Å^{-1}.

This inequality agrees with the estimate $\Delta k \approx 0.032$ Å^{-1}, which can be obtained from the angular dependence of the area of the neck in the range 0–5° from the [100] direction, measured in [9].

Figure 9 shows the cross section of the electron "jack" in the (110) plane, constructed from the entire set of our data; the letters indicate which lines were used for the determination of a given dimension. For example, the dimension of the electron octahedron along the $[1\bar{1}0]$ direction is determined by the lines g′ and g″ (Figs. 5, 6).

Establishment of the shape of the spheroids and lenses is made difficult by the fact that a center of symmetry is lacking in these figures. Although the dimension e_2 is determined from the noncentral cross section, the construction of the spheroid is made easy by the fact that the line i was determined experimentally. Basing our treatment on these experimental points and the extremal dimension $2e_2$, we succeeded in estab-

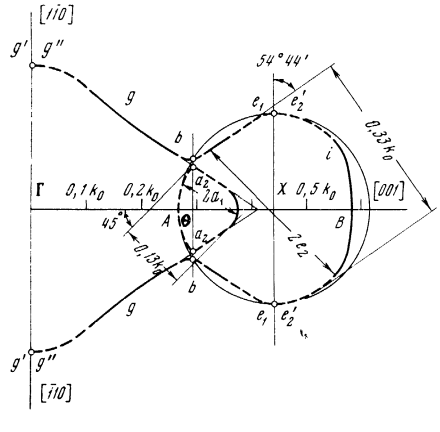

FIG. 9. Central cross section of the electron surface with the (110) plane. Solid lines and separate points (○) are the result of the experiment.

lishing the part of the cross section of the spheroid in the vicinity of the neck. The existence of the line e in the angular range 45–75° allows us to extend the construction even further; however, since the experimental points belonging to the line i terminate at an angle 14° to the [001] direction (center at the point Γ), this part of the spheroids is drawn on the diagram with dashed lines. The complete cross section of the spheroid was obtained by extrapolation. The size at the angle 54°44' (value of $2e_2''$ from the diagram of Fig. 6) supports its validity.

In the construction of the cross section of the lens, we have used several additional assumptions.

We shall assume that the electron "jack" was formed by the intersection of the octahedron with spheres. Then the center of the sphere X, which lies on the line ΓB, can be determined with small error as the point of intersection of the line ΓB with the circle of radius e_1X, drawn from the point b. The distance Θb is known to us from experiment, as is the distance from the end of the spheroid to the neck BΘ. It is natural to suppose that the extremal cross section of the lens for H ∥ [001] lies in the plane of the neck and consequently the point Θ, which is the point of intersection of the plane of the neck with the ΓB axis, will simultaneously be the center of this cross section. The distance Θa_2 corresponds to the experimental value of the radius of the lens. We shall draw the circle with the radius Xe_1 with center at the point X and lay off from the point A the length of the lens, determined from the diagram of Fig. 4 (the dimension $2a_1$, along [001]). If we now lay off a series of extremal dimensions $2a_1$ and carry out the corresponding extrapolation, we shall obtain the cross section of the lens shown in Fig. 9. The area of such a cross section is $S_{(110)} = 0.048$ Å^{-2}, which agrees with the result $S_{(110)} = 0.049$ Å^{-2} (known from [9]) within the range of experimental error. Although the point A was chosen by us with some degree of arbitrariness, nevertheless such a shape of the lens describes our experimental results well, better than a shift of the point A to the left or the right with conservation of all the experimental dimensions leads to a significant increase or decrease in the area.

The fundamental experimental dimensions of the electron "jack" and the lenses and their comparison with the theoretical calculation of Loucks are given in the table. The area of the cross section of the electron "jack" in the (111) plane $S_{(111)} = 0.81$ Å^{-2}, which is somewhat greater than the result $S_{(111)} = 0.79$ Å^{-2} from [12] and less than the value of Girvan and Gold $S_{(111)} = 0.9$ Å^{-2} known from [10]. The total area of the surface of the electron "jack" and the lenses, computed from the results of our measurements, is equal to 12.5 Å^{-2} and their volume is $V = 1.55$ Å^{-3}.

In the direction of the magnetic field along [111], the extremal orbit on the central part of the electron "jack" has the form of a hexagon similar to the orbit on the central part of the hole octahedron. By using the value of the effective mass in this direction, from [20], we can calculate (by means of Eq. (2)) the value of the mean velocity of the electrons on this orbit: $\bar{v}_e = 0.60 \times 10^8$ cm/sec.

CONCLUSION

Thus, as a result of the study of the radio-frequency size effect, experimental information has been obtained on the shape and dimensions of the Fermi surface of molybdenum. The experimental results confirmed the validity of the theoretical model suggested. However, it must be noted that the dimensions of the electron surface and the hole ellipsoids are, according to experiment, somewhat larger than follows from the calculation of Loucks, while the dimensions of the hole octahedron are smaller.

The absence of closed orbits, which were not discovered by us or by other investigators,[20,22] testifies to the existence of a gap between the hole octahedron and the electron "jack" along ΓH. The value of this gap (see the table) $\Delta k = 0.05 \pm 0.04$ Å^{-1} amounts to 2.5% of $k_0 = 1.998$ Å^{-1}. As is seen from the table, the agreement of our experimental results with the results of the investigations by other methods is rather good.

Basing our arguments on the given data and the knowledge of the theoretical model, we constructed an experimental model of the Fermi surface of molybdenum. We give the values of the total area of the surface of such a model and the volumes of its electron and hole parts:

Total electron volume:		1.55 Å^{-3}
Total hole volume:		1.51 Å^{-3}
Total area of the surface	Experiment	24.1 Å^{-2}
	Model of [13]	23.93 Å^{-2}

The experiment confirms the complete compensation of these volumes. The total volume of the surface computed from the experimental results agrees with the theoretical value. It differs from the data of Sparlin and Marcus[9] and, although the difference actually lies within the limits of experimental accuracy, nevertheless it is justified by the insufficiently complete knowledge to the authors of [9] of the shape and dimensions of the large cross sections of the electron surface.

The authors are sincerely grateful to V. F. Gantmakher for a detailed discussion and a number of valued observations, to M. I. Kaganov and É. A. Kaner for attention and interest in the work, to G. P. Kovtun for the loan of pure molybdenum, to K. I. Elistratova for orientation of the samples, and to I. A. Labazev for technical assistance.

[1] E. Fawcett and D. Griffiths, J. Phys. Chem. Sol. 23, 1631 (1962).
[2] E. Fawcett, Phys. Rev. Lett. 7, 26 (1961).
[3] E. Fawcett, Phys. Rev. 128, 154 (1962).
[4] W. M. Lomer, Proc. Phys. Soc. (London) 80, 489 (1962).
[5] W. M. Lomer, Proc. Phys. Soc. (London) 84, 327 (1964).
[6] J. H. Wood, Phys. Rev. 126, 517 (1962).
[7] G. B. Brandt and J. A. Rayne, Phys. Rev. 132, 1945 (1963).
[8] W. M. Walsh and C. C. Grimes, Phys. Rev. Lett. 13, 523 (1964).
[9] D. M. Sparlin and J. A. Marcus, Phys. Rev. 144, 484 (1966).
[10] C. K. Jones and J. A. Rayne, Phys. Lett. 8, 155 (1964).

[11] C. K. Jones and J. A. Rayne, LT9, Proc. IX Inter. Conf. Columbus, Ohio, 1964, Part B, New York, Plenum Press, 1965, p. 790.
[12] A. Myers and G. Leaver, Proc. X Inter. Conference of Low Temperature Physics, 3 VINITI, 1967, p. 290.
[13] T. L. Loucks, Phys. Rev. **139** 4A, 1181 (1965).
[14] V. F. Gantmakher, Zh. Eksp. Teor. Fiz. **44**, 811 (1963) [Sov. Phys.-JETP **17**, 549 (1963)].
[15] É. A. Kaner and V. F. Gantmakher, Usp. Fiz. Nauk **94**, 193 (1968) [Sov. Phys.-Uspekhi **11**, 81 (1968)].
[16] V. V. Boĭko, V. A. Gasparov, and I. G. Gverdtsiteli, ZhETF Pis. Red. **6**, 737 (1967) [JETP Lett. **6**, 212 (1967)].
[17] N. J. Hopkins, Rev. Sci. Instr. **20**, 401 (1949).
[18] I. P. Krylov and V. F. Gantmakher, Zh. Eksp. Teor. Fiz. **51**, 740 (1966) [Sov. Phys.-JETP **24**, 492 (1967)].
[19] A. Fukumoto and H. W. P. Strandberg, Phys. Lett. **23**, 200 (1966).
[20] R. Herrmann, Phys. Stat. Sol. **25**, 427 (1968).
[21] V. F. Gantmakher and I. P. Krylov, Proc. X Inter. Conference on Low Temperature Physics **3**, VINITI, 1967, p. 128.
[22] E. Fawcett and W. A. Reed, Phys. Rev. **134**, A723 (1964).

Translated by R. T. Beyer
62